Two essential regions for tRNA recognition in *Bacillus subtilis* tryptophanyl-tRNA synthetase

Jie JIA, Feng XU, Xianglong CHEN, Li CHEN, Youxin JIN[1] and Debao T. P. WANG

State Key Laboratory of Molecular Biology, Institute of Biochemistry and Cell Biology, Shanghai Institutes for Biological Sciences, Chinese Academy of Sciences, Shanghai 200031, People's Republic of China

Bacillus subtilis tryptophanyl-tRNA synthetase (TrpRS) is a homodimeric enzyme. A model for its ability to recognize $tRNA^{Trp}$ in *B. subtilis* was proposed by using computer modelling. This was based on the the fact that there is high homology among bacterial TrpRSs [Chen, Jiang, Jin and Wang (2001) Acta Biochim. Biophys. Sinica **33**, 687–690], in which the enzyme dimer binds to two $tRNA^{Trp}$ molecules and each $tRNA^{Trp}$ is bound to two different domains across the surface of the dimer. In this work, three deletion mutants of TrpRS were constructed and their products were purified. After determining the kinetic parameters of the mutants in the two-step reaction, it was found that the relative activities of wild-type and mutant enzymes had changed little in the ATP-pyrophosphate exchange reaction. In contrast, the activities of three mutant proteins were much decreased in the $tRNA^{Trp}$ aminoacylation assay. Deletion of residues 108–122 and residues 234–238 caused 44 % and 80 % reductions in the activity, respectively. When both regions were deleted, the aminoacylation activity of the TrpRS mutant was too low to be determined using $tRNA^{Trp}$ at the limiting concentration. Gel-retardation assays showed that the acceptor minihelix and the anticodon microhelix were recognized by the domains of TrpRS spanning residues 108–122 and residues 234–238 respectively. In addition, the deletion of amino acids 234–238 affected the normal induced expression of TrpRS at 37 °C. In conclusion, residues 108–122 and 234–238 were found essential for $tRNA^{Trp}$ recognition.

Key words: acceptor minihelix, anticodon microhelix, $tRNA^{Trp}$-binding domain.

INTRODUCTION

Correct recognition of tRNA by aminoacyl-tRNA synthetase (aaRS) is fundamental to the fidelity of protein synthesis. In recent years, the focus has been on analysing the structure of aaRSs and identifying the sequence determinants responsible for specific recognition of cognate tRNA and amino acids by aaRSs. The aaRSs catalyse the attachment of an amino acid to its cognate tRNA in a highly specific two-step reaction. Structural and functional studies of numerous aaRSs have shown that these enzymes are composed of distinct domains with clearly defined roles in substrate recognition and catalysis [1].

aaRSs are divided into two classes based on the sequences and structures of their active-site domains [2–4]. The structures of the aaRSs consist of two major domains that interact with the two domains in the secondary structure of tRNA; the acceptor • TψC stem-loop and the anticodon • D stem-loop [5–10]. This secondary structure forms an L-shaped tertiary fold where one domain (acceptor • TψC minihelix) is formed by the coaxial stacking of the 5 bp TψC stem onto the 7 bp acceptor helix [9,11,12]. The older, and highly conserved, catalytic domain of synthetase interacts with the acceptor • TψC minihelix and is responsible for catalysing amino acid attachment. The second, idiosyncratic and more recent, domain of the synthetase interacts with the anticodon arm of the tRNA [13]. Our understanding of these interactions has been greatly enriched by the availability of high-resolution crystal structures for the majority of aaRSs [1].

Tryptophanyl-tRNA synthetase (TrpRS) belongs to the class I aaRS family that contains catalytic signatures with consensus amino acid sequences, HIGH and KMSKS [14,15]. The members of this family have a Rossmann fold that binds ATP [3], and catalyses the acylation at the 2′-OH position of the ribose of the CCA end of tRNA. Since TrpRS is a dimeric enzyme that contains the smallest subunit chains among known aaRSs, it has been considered as an ideal candidate for structure–function studies by means of site-directed mutagenesis [16–20]. The previously determined crystal structure of ligand-free TrpRS at 2.9 Å (1 Å ≡ 0.1 nm) and TrpRS: tryptophanyl-5′AMP (TAM) complex showed the potential substrate-binding domains and the domain movements in the aminoacylation process [16,17].

Bacillus subtilis TrpRS is a homodimeric enzyme, each subunit being 330 amino acids long. Its gene was cloned into the pUC8 plasmid and then inserted into the pKK223-3 vector to form a high-level expression plasmid named pKSW1 [21,22]. Furthermore, site-directed mutagenesis of the *trpS* gene was carried out and insight into the structure–function relationship of this enzyme was gained from characterizing the respective gene products [18,19,23]. Though there were data available about the crystal structures of TrpRS and its TAM complex [16,17,24], the $tRNA^{Trp}$-binding domain in the TrpRS and the mechanism of $tRNA^{Trp}$ recognition were still elusive. It was known that the amino acid sequence of the *B. subtilis trpS* was 55.8 % homologous to that of *Escherichia coli* and 78.1 % to that of *Bacillus stearothermophilus*, so we used the data from *B. stearothermophilus* TrpRS as a template in constructing the model of *B. subtilis* TrpRS. With the software PMODELLING (designed by the Shanghai Institute of Biochemistry and Cell Biology, Shanghai, China), we predicted the homologous model of *B. subtilis* TrpRS [25] and found within *B. subtilis* TrpRS two putative binding regions to $tRNA^{Trp}$ (Figure 1). The first region, residues 108–122, lies within the Rossmann fold, bordering the tryptophan-binding site. The second region,

Abbreviations used: aaRS, aminoacyl-tRNA synthetase; IPTG, isopropyl β-D-thiogalactoside; SD, small domain; TAM, TrpRS:tryptophanyl-5′AMP; Trp-AMP, tryptophanyl-5′-AMP; TrpRS, tryptophanyl-tRNA synthetase; wt, wild-type.

[1] To whom correspondence should be addressed (e-mail yxjin@sunm.shcnc.ac.cn).

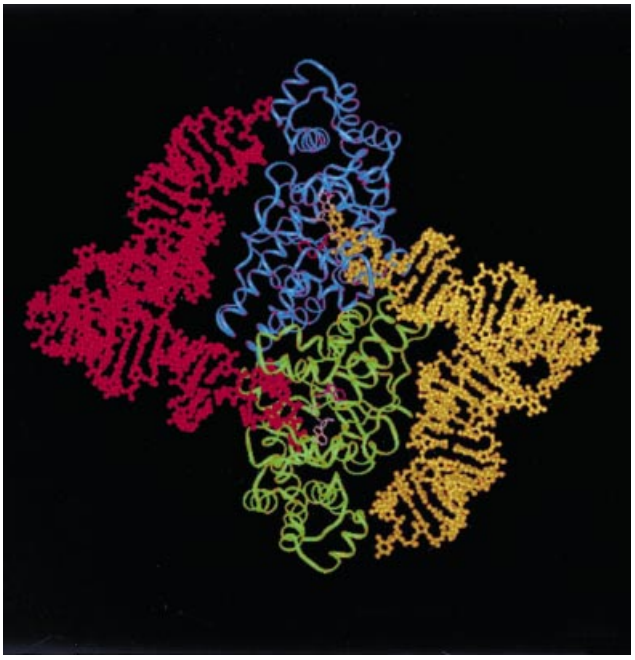

Figure 1 Putative binding of tRNA^{Trp} with *B. subtilis* TrpRS

The two tRNA^{Trp} are coloured red and yellow. *B. subtilis* TrpRS subunits are coloured blue and green. The moiety highlighted in white is AMP and in purple is the Trp moiety. Binding of tRNA occurs across the dimer interface. Each tRNA molecule interacts across a dimer, the amino acid acceptor stem of L-shaped tRNA binds to the 108–122 domain in one subunit and the anticodon loop binds to the 234–238 domain in the other subunit.

residues 234–238, lies within the small domain (SD), opposite the extended-chain-containing residues. We cloned, expressed and purified three variants of *B. subtilis* TrpRS, in which the different potential tRNA^{Trp} binding regions were deleted, so as to study the interaction between tRNA^{Trp} and TrpRS of *B. subtilis*. These mutants could be used to directly test their binding activity with tRNA^{Trp} and to compare their kinetic parameters with that of TrpRS wild-type (wt) in the aminoacylation reactions.

MATERIALS AND METHODS

Sequence-homology analysis

Sequence analysis was performed on *E. coli*, *B. stearothermophilus*, *B. subtilis*, *Homo sapiens* and *Haemophilus influenzae* TrpRS using the software Clustal X. The crystal structure of *B. subtilis* was modelled using the software PMODELLING (designed by Shanghai institute of Biochemistry and Cell Biology), based on the crystal structure of *B. stearothermophilus* as described previously [17].

Domain-deletion mutagenesis of *B. subtilis trpRS* gene

Three deletion mutants named pKSWJ1, pKSWJ2 and pKSWJ1L15 were constructed from a commercial plasmid, pKK223-3 (Amersham Biosciences, Little Chalfont, Bucks, U.K.). The plasmids pKSWJ1 and pKSWJ2 harboured the mutant *B. subtilis trpRS* gene, lacking 108–122 amino acids and 234–238 amino acids in the wt enzyme, respectively; the pKSWJ1L15 was a double mutant lacking both 108–122 and 234–238 regions. Each deletion mutagenesis involved a three-step PCR, as described previously [26]. We specifically designed six primers for generating these deletions. Their sequences were as follows: primer 1, 5′-GCGAATTCATGAAACAAACGATTTTTTC-3′ (including an *Eco*RI site, underlined); primer 2, 5′-ATGTTAACAGAGTCATCCGCTCAAGCTCG-3′; primer 3, 5′-GAGCGGATGACTCTGTTAACATATCCGCCGCTGAT-3′; primer 4, 5′-TCGGAATTCGAATCAAAGGTCAACTGAAAA-3′ (also including an *Eco*RI site); primer 5, 5′-AAGGTTGGAAACCTTATCAAATTTGACAATGCCTTC-3′; primer 6, 5′-AAATTTGATAAGGTTTCCAACCTTCTTACAATTTATTCA-3′. All mutant sequences were confirmed by sequencing.

Protein expression and purification

The plasmid pKSWJ1, pKSWJ2 and pKSWJ1L15 were transformed into *E.coli* JM109 and the bacteria were cultured and induced to express the mutant TrpRS proteins, as described previously [23]. The expression level was checked by running SDS/polyacrylamide gels, stained with Coomassie Blue. These mutants showed different temperature-dependent expression profiles under isopropyl-β-D-thiogalactoside (IPTG) induction. The best yield for pKSWJ1 was achieved at 37 °C and for pKSWJ2 and pKSWJ1L15 at 25 °C. The cells were pelleted by centrifugation.

The pellets were washed twice with 50 mM Tris/HCl (pH 7.2) and stored at −80 °C. After resuspending in buffer A [20 mM potassium phosphate (pH 7.5), 1 mM EDTA, 5 mM 2-mercaptoethanol, 10 % (v/v) glycerol and 1 mM PMSF], cells were sonicated on ice and the sludge was centrifuged at 4 °C and 20000 ***g*** for 30 min. Streptomycin sulphate (1 %) was added to the supernatants and the nucleic acids were precipitated by incubating on ice for 10 min with periodic mixing, before centrifugation at 4 °C and 39000 ***g*** for 30 min. The resulting supernatants were further purified on DEAE Sepharose™ Fast-Flow columns (Amersham Pharmacia Biotech) to electrophoretic homogeneity. The TrpRS proteins were concentrated with polyethylene glycol 6000, dialysed for 10 h against buffer B [as buffer A, but with 50 % (v/v) glycerol and pH 6.8] and stored at −80 °C. Enzyme concentrations were determined as described previously [27].

In vitro transcription of tRNA^{Trp}

The tDNA^{Trp} was synthesized with a Beckman Oligo 1000 M DNA/RNA Synthesizer, and made into double-stranded templates with PCR. The primer sequences were as following: primer A, 5′-CTCTAATACGACTCACTATAAGGGGCATAGTTAACGGTA-3′ (containing the T7 RNA polymerase promoter); primer B, 5′-TCCCAAGCTTCCTGGCAGGGGCAGTAGGAA-3′ (containing an *Bst*OI site underlined). The double stranded DNAs digested by *Bst*OI were directly employed as *in-vitro*-transcription templates, using RiboMAX™ Large Scale RNA Production Systems (Promega, Madison, WI, U.S.A.). Full-length transcripts were isolated by preparative PAGE (29:1, monoacrylamide/bisacrylamide, containing 8 M urea). The desired band was cut out under UV light and tRNA^{Trp} was recovered in a buffer containing 0.5 M ammonium acetate, 10 mM magnesium acetate, 1 mM EDTA (pH 8.0), 0.1 % (w/v) SDS, overnight. The suspension was centrifuged at 4 °C and 19500 ***g*** for 30 min, and the supernatant was ethanol precipitated, resuspended in sterile water and stored at −20 °C. Concentrations were determined by measuring absorbances at 260 nm. Before the aminoacylation assay, transcripts were heated to 70 °C for 2 min and allowed to cool to 25 °C.

PP_i-ATP exchange activity assay

The tryptophanyl adenylate synthesis was measured by the [γ-^{32}P]ATP-PP_i exchange assay at 25 °C as described previously [24]. Kinetic analysis was performed with variable concentrations of ATP or tryptophan. The wt enzyme was used as positive control, whereas Gly was used as negative control. All the enzymes in the reactions were at a final concentration of 0.7 μM. The radioactivity results were revealed and quantified using a PhosphorImager™ (Molecular Dynamics, Little Chalfont, Bucks, U.K.). Each assay was repeated at least four times. Data were used to make plots of the reaction velocity (V) against the substrate concentration [S], and to calculate the K_m and V_{max} values for ATP and Trp.

Aminoacylation kinetics

Aminoacylation assays of $tRNA^{Trp}$ were performed as described previously at 22 °C in a reaction buffer consisting of 4 mM ATP, 0.8 mM dithiothreitol, 1 μCi L-[5-^{3}H]tryptophan, 8 mM $MgCl_2$, 80 mM Tris/HCl (pH 7.5), 0.02 μM *B. subtilis* $tRNA^{Trp}$ transcribed *in vitro*, in a total volume of 50 μl [28]. After 30 min, 10 μl aliquots were spotted on Whatmann 3 MM filter discs, which were washed three times with ice-cold 5 % trichloroacetic acid containing 0.05 % tryptophan, and with cold 95 % ethanol, dried, and transferred to vials for determination of radioactive counts. For all kinetic assays the concentrations of Trp and $tRNA^{Trp}$ varied over at least a 10-fold range. [$tRNA^{Trp}$] varied from 0.04 μM–2.56 μM while [Trp] was constant at 8 μM; and [Trp] was varied between 0.5 μM–8 μM while [$tRNA^{Trp}$] was kept at 10 μM. Each process was repeated at least three times under the same conditions. Kinetic parameters (k_{cat} and K_m) for aminoacylation were calculated from Eadie–Hofstee plots; all data were fitted to the Michaelis–Menten equation.

Gel-retardation assay

Enzyme–tDNA interactions were assayed using a band-shift assay as described previously [29]. The substrates, $tDNA^{Trp}$ acceptor minihelix (5′-AGGGGCAGTGGGTTCGATTCC-TACTGCCCCTGCCA-3′) and anticodon microhelix (5′-GAG-GTCTCCAAAACCTC-3′), were synthesized and labelled with [γ-^{32}P]ATP using T4 Polynucleotide Kinase (MBI, Vilnius, Lithuania). The labelled minihelix or microhelix was ethanol precipitated, resuspended in sterilized water and stored at −20 °C. The TrpRS (wt) and the three mutants were incubated with 40 pmol of radiolabelled tRNA elements in an 11 μl volume containing 20 mM Tris/HCl (pH 7.5), 150 mM NaCl, 10 mM $MgCl_2$, 10 mM 2-mercaptoethanol, 10 % (v/v) glycerol and 0.1 mg/ml BSA. The concentrations of various TrpRSs were kept at 4 μM. After incubation at 25 °C for 20 min, the mixture was placed on ice and loaded on to a 6 % polyacrylamide gel (mono/bis, 29:1) containing 5 % (v/v) glycerol in 0.5 × Tris/borate/EDTA (1 × TBE = 45 mM Tris/borate/1 mM EDTA) at 4 °C. After electrophoresis, the gel was fixed, dried and subjected to autoradiography.

RESULTS

Analysis of conservation of TrpRS in varied species

We aligned the sequences of bacterial TrpRSs with the software Clustal X, and found them to be highly homologous. In particular, the sequence of *B. subtilis* TrpRS was 78.1 % homologous to that of *B. stearothermophilus*. The conserved residues were mapped not only in the HIGH and KMSKS class-defining motif (residues G18, K193, M194, S195 and S197 in the *B. subtilis* enzyme) but also in other regions (residues G8, D42, G70, A132, P143, D147, R156, A159 and K270), suggesting that the crystal structure of *B. subtilis* TrpRS might be similar to that of *B. stearothermophilus* TrpRS. Based on the crystal structure of *B. stearothermophilus* TrpRS (the set of parameters was a gift from Professor C. W. Carter, Jr), we constructed a series of *B. subtilis* TrpRS structural models with the software PMODELLING. In the ligand-free TrpRS model, the Trp92 was buried among the subunits and served as a crucial residue participating in inter-subunit conformational changes upon tryptophanyl-5′-AMP (Trp-AMP) formation, which in turn induced within *B. subtilis* TrpRS a pocket enclosing Trp-AMP. The pocket was composed of residues G8, I9, Q10, M130, V144, D147, Q148, M194, S195 and K196. In *B. stearothermophilus* TrpRS, this pocket was reported to be near the tRNA-binding domain, where the tryptophanyl group was transferred conveniently from Trp-AMP to $tRNA^{Trp}$ in the aminoacylation reaction. The model for $tRNA^{Trp}$ recognition by *B. subtilis* TrpRS was deduced from the model of $tRNA^{Tyr}$ recognition by *B. stearothermophilus* TyrRS, taking into account the similarity in the crystal structures of *B. stearothermophilus* TrpRS and TyrRS ([17], Figure 1). $tRNA^{Trp}$ binds across the dimer interface of the homodimeric TrpRS, one domain of $tRNA^{Trp}$ docking in one subunit and the second domain in the other identical sister subunit. Consequently, we identified two domains from the sequence alignments of the two $tRNA^{Trp}$ binding sites in TrpRSs among *E. coli*, *B. stearothermophilus*, *B. subtilis*, *H. sapiens* and *H. influenzae* (Figure 2). One was the residues 108–122 domain, named the acceptor-binding loop, which interacted with the amino acid acceptor stem of $tRNA^{Trp}$; the other was the residues 234–238 domain, named the anticodon-binding loop, which recognized the anticodon loop and anticodon CCA. Both these domains were situated on flexible loops in the *B. subtilis* TrpRS and exposed to the surface; the acceptor-binding loop was near the binding pocket around the Trp-AMP as we previously predicted.

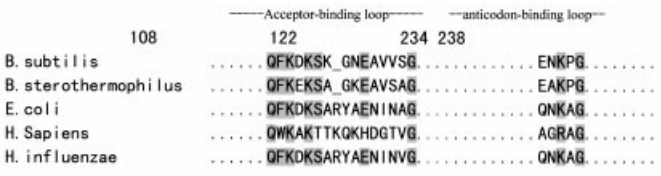

Figure 2 Comparison of the amino acids of two binding domains

The homology analysis of the predicted $tRNA^{Trp}$ binding domains in tryptophanyl-tRNA synthetase of *B. subtilis, B. sterothermophilus, E. coli, H. Sapiens* and *H. influenzae*. Conserved residues of TrpRS are shaded in grey.

Purification and characterization of *B. subtilis* TrpRS and its mutants

In order to study the two tRNA-binding regions identified above, we have successfully constructed three mutant *trpS* genes: pKSWJ1 deleting amino acids 108–122, pKSWJ2 deleting amino acids 234–238, and pKSWJ1L15 lacking both regions. Cultures were incubated at different temperatures, 25 °C or 37 °C, to overexpress soluble proteins. It was found that the deletion of amino acids 108–122 had no effect on the expression of TrpRS, but the deletion of only five amino acids, residues 234–238, had a strong negative effect on the expression. TrpRS was expressed as an inclusion body in the strains containing pKSWJ2 or

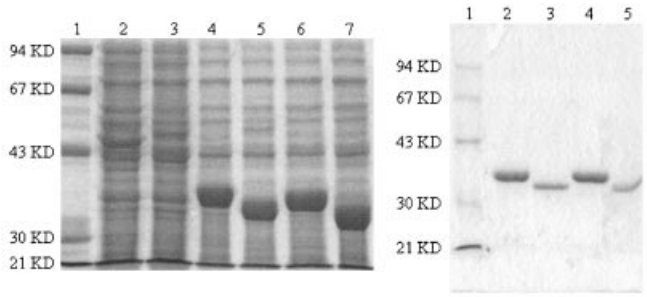

Figure 3 Expression analysis of the three TrpRS mutants

Electrophoretograms of SDS (0.1%)/PAGE (12% gel). Left-hand panel: lane 1, standard protein marker (21–94 kDa); lane 2, *E. coli* JM109 strain; lane 3, JM109 (pKK223-3); lane 4, JM109 (pKSW1); lane 5, JM109 (pKSWJ1); lane 6, JM109 (pKSWJ2); lane 7, JM109 (pKSWJ1L15). JM109 (containing pKSW1 or pKSWJ1) was grown at 37 °C, but JM109 (containing pKSWJ2 or pKSWJ1L15) was incubated at 25 °C, in Luria–Bertoni medium in the presence of 50 μg/ml ampicillin. At $A_{550} = 0.7$, IPTG was added to a final concentration of 1 mM. Right-hand panel (purified enzymes): lane 1, standard protein marker (21–94 kDa); lane 2, pKSW1; lane 3, pKSWJ1; lane 4, pKSWJ2; lane 5, pKSWJ1L15.

pKSWJ1L15 at 37 °C under IPTG induction, but we demonstrated that the enzymes could be expressed as soluble proteins at 25 °C. The overexpression of TrpRS was confirmed by SDS/PAGE and the overexpressed proteins appeared as a strong band of around 35 kDa (Figure 3). After single-step purification with a DEAE Sepharose™ Fast Flow column, the purity of the enzyme was shown to be over 90% as determined by gel scanning.

ATP-pyrophosphate exchange

To assess the abilities of TrpRSs to catalyse the formation of Trp-AMP in the first step of aminoacylation, we obtained the kinetic data of 3 mutants using [γ-^{32}P]ATP as described previously [24]. [γ-^{32}P]ATP and [^{32}P]PP$_i$ were separated by polyethyleneimine-cellulose chromatography in an exchange assay containing 0.7 μM of the purified enzyme (Figure 4), and the activity was demonstrated by autoradiography. The kinetic parameters were calculated on the initial rate of the PP$_i$-ATP exchange followed by nonlinear regression fitting to the Michaelis–Menten equation. The enzymes showed very little difference in their relative activities (results not shown). The TrpRS (wt) exhibited slightly more activity than pKSWJ1, pKSWJ2 and pKSWJ1L15 when the concentration of Trp was kept at 2 mM and the ATP concentration was varied between 0.04–4 mM. However the relative activities showed a converse result, k_{cat}/K_m of TrpRS (wt) is lower than that of the mutants when the Trp concentration was varied and ATP was kept at a constant concentration of 4 mM. All the changes between the wt and the mutant proteins were negligible, however, in comparison with the changes in activities of the secondary step of tRNA aminoacylation. These data demonstrated that the deletion of one of the two regions, or both regions, has little effect on the first step in tRNA aminoacylation.

Recognition between tRNA^{Trp} and the mutant TrpRS

To further address the difference between TrpRS (wt) and the three mutants we generated, we explored the recognition between tRNA^{Trp} and TrpRSs. tRNA molecules prepared by transcription *in vitro* do not contain the modified nucleotides found in natural

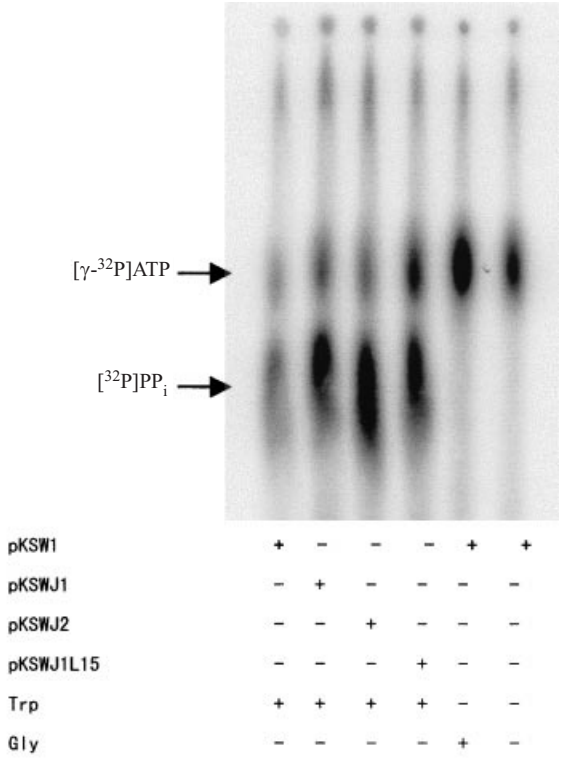

Figure 4 ATP-PP$_i$ exchange assay

The assay was carried out with purified TrpRS (pKSW1) and TrpRS mutants (pKSWJ1, pKSWJ2 and pKSWJ1L15) with samples incubated for 30 min at 25 °C and additions (+) as indicated. When the ATP-PP$_i$ exchange reaction was complete, the [^{32}P]PP$_i$ was separated as a product on a polyethyleneimine-cellulose chromatogram and revealed by autoradiography. The position of the [^{32}P]PP$_i$ and [γ-^{32}P]ATP are marked with arrows.

tRNAs. Despite this fact, most tRNA transcripts are efficient substrates for their cognate synthetases [30,31]. The kinetic parameters were measured from the dependence of the initial rate of the tRNA aminoacylation on tryptophan and ATP concentrations, as shown in Table 1. In the $1/v - 1/[S]$ plot the mutants showed different reduced recognition activities, but because of the limited concentration of transcripted tRNA *in vitro*, some data could not be determined. While the K_m value of TrpRS (pKSWJ1) was lower than that of TrpRS (pKSWJ2), the K_m values of both were not much higher than that of TrpRS (wt). Even the K_m value of TrpRS (pKSWJ2) was just 2.9-fold higher than that of TrpRS (wt), and the k_{cat}/K_m value was 4.5-fold lower than that for TrpRS (wt). However, when both amino acid regions 108–122 and 234–238 were deleted from TrpRS, aminoacylation activity became very weak and difficult to determine (Table 1).

Protein-tDNA binding assay

We used the protein-tDNA binding assay to confirm the importance of the two regions identified as essential for the second step of aminoacylation. Autoradiography showed that the wt TrpRS (pKSW1) bound to both tRNA^{Trp} element analogues (minihelix and microhelix). But the TrpRS mutant from pKSWJ1 (108–122 deletion) was unable to recognize the tRNA^{Trp} minihelix (acceptor stem). A very similar result was obtained for the

Table 1 Kinetic parameters of $tRNA^{Trp}$ aminoacylation

Each assay was carried out at least for three times under the same conditions. Kinetic parameters (k_{cat} and K_m) for aminoacylation were calculated from Eadie–Hofstee plots; all data were fitted to the Michaelis–Menten equation. When the concentration of one substrate was changed, that of the other was kept at a saturating concentration. [$tRNA^{Trp}$] was changed from 0.04 to 2.56 μM when [Trp] was constant at 8 μM. When [Trp] was varied between 0.5 and 8 μM, [$tRNA^{Trp}$] was kept at 10 μM. nd, not determined. K_m are means $\pm$ S.D.

	$tRNA^{Trp}$			Trp		
Enzyme forms	K_m (μM)	k_{cat} (s^{-1})	k_{cat}/K_m ($s^{-1} \cdot \mu M^{-1}$)	K_m (μM)	k_{cat} (s^{-1})	k_{cat}/K_m ($s^{-1} \cdot \mu M^{-1}$)
pKSW1 (wt)	0.18 ± 0.01	0.90	5.02	0.73 ± 0.06	0.90	1.24
pKSWJ1 (108–122 deletion)	0.22 ± 0.01	0.61	2.78	2.12 ± 0.04	0.61	0.29
pKSWJ2 (234–238 deletion)	0.52 ± 0.03	0.59	1.13	2.34 ± 0.01	0.59	0.25
pKSWJ1L15 (double deletion)	nd	nd	nd	2.38 ± 0.11	0.40	0.17

mutant protein missing amino acids 234–238 (encoded by plasmid pKSWJ2), which showed a very low affinity for the microhelix (anticodon loop, Figure 5b). These results were in agreement with our prediction from the computer modelling (see 'Analysis of conservation of TrpRS in varied species'). Therefore, we concluded that the 108–122 residues were responsible for the recognition of $tRNA^{Trp}$ acceptor stem, and the 234–238 residues interacted with the $tRNA^{Trp}$ anticodon loop. In addition, each $tRNA^{Trp}$ should bind both the subunits and each terminus of the L-shaped tRNA bound to different domains in the protein.

DISCUSSION

TrpRS is the smallest protein in the family of bacterial tRNA synthetases. It is an ideal model to study the interaction between tRNA and enzyme in the process of aminoacylation. TrpRS is composed of two identical subunits. Sequence-homology analysis finds that the sequences of TrpRSs are highly conserved in bacteria such as *E. coli*, *B. stearothermophilus* and *B. subtilis* [22,28]. *B. stearothermophilus* TrpRS was used as a template to predict the structure of *B. subtilis* TrpRS (because of more than 78.1 % homology) through homology modelling in our study. It was demonstrated that the synthetase has 16 α-helices and five β-sheets in one unit in this model (Figure 1). The only tryptophan Trp92 was located on the interface of subunits, which was reported to be a crucial part of a network of connectivity between the two subunits.

In our previous work [28], it was shown that the major identical elements of *B. subtilis* $tRNA^{Trp}$ are anticodon bases C34, C35, A36 and G73; the minor elements are G5–C68 and A9. Trp-5′-AMP binds to an obvious binding pocket, composed of G8, I9, Q10, M130, V144, D147, Q148, M194, S195 and K196 in TrpRS [25]. The binding of the tRNA acceptor stem to TrpRS should be near the site which connects with Trp-AMP, because the environment would help to transfer the acyl group from AMP to tRNA. The average distances from anticodon to acceptor-binding loop in all tRNA molecules, based on the crystal structures solved, are from 50–70 Å. The distance from Trp in one active site to any residues in same subunit is not more than 41.37 Å, which is not far enough to contain a whole $tRNA^{Trp}$ molecule. So the $tRNA^{Trp}$ should bind over the subunits. Two loops in the w-shaped *B. subtilis* TrpRS were shown to connect with the L-shaped tRNA molecule. This study showed that TrpRSs from various species shared high homology (Figure 2), residues 108–122 and residues 234–238 in particular. These two short regions, in one subunit, were predicted to bind to acceptor stem and anticodon of variant $tRNA^{Trp}$. These predictions were in agreement with the conclusion from the 2.9 Å crystal structure of *B. stearothermophilus* ligand-free tryptophanyl-tRNA synthetase [17]. By using Ramachandran angle difference plots, these two regions were implicated in binding of cognate tRNA in work by Carter and colleagues [17]. The first, residues 117–119, lies within the Rossmann fold, bordering the tryptophan-binding site. The sequences were thought to be an acceptor-binding domain. The second, residues 233–237, lies within the SD, opposite to the extended-chain containing residues homologous to the segment in GlnRS that interacts with the U35 of the glutamine anticodon.

In our homology modelling, because these two regions were located on flexible loops, it was predicted that their deletions would not affect the whole structure of *B. subtilis* TrpRS and consequently the active sites of TrpRS would stay intact. The binding of $tRNA^{Trp}$, however, would be affected dramatically. To test this model, the kinetics parameters of the ATP-PP_i exchange reaction were calculated using TrpRS (wt) and its three mutants lacking these regions. The relative activities showed that the mutant proteins had only slightly more affinity to Trp and slightly less affinity to ATP. Therefore, the deleting of these two regions did not affect the ATP-PP_i exchange reaction substantially, consistent with the model prediction.

From the analysis of sequence homology, residues 108–122 were predicted to be an acceptor-binding loop, and residues 234–238 to be related to the interaction with the $tRNA^{Trp}$ anticodon. The individual deletion of residues 108–122 or 234–238 reduced tRNA aminoacylation efficiency to 44 % and 80 % respectively, compared with TrpRS (wt). However, the double deletion led to a much more decreased aminoacylation efficiency, and the very low $tRNA^{Trp}$ affinity to this mutant protein made the kinetic parameters difficult to determine. This can be explained as follows. An L-shaped tRNA molecule binds to two sites in different subunits, across the dimer interface, with each of the binding sites contributing partially to the stability of tRNA–TrpRS complex. Consequently, the individual deletions only induce partial loss of activity. When one binding region is deleted, the other region is still bound to the tRNA, but the stability is affected. It is hypothesized that tRNA would not only bind to these two sequences, but that each domain of tRNA may bind to a positive pocket, mainly composed of residues 108–122 or 234–238, with minor help from other residues which could equilibrate the polarity in the binding pocket. CD spectra indicated that the mutants had some loss in the secondary structure of the enzyme (results not shown), but this was unlikely to cause significant changes in the activities of aminoacylation, because of the similar spectra for all three mutants. Once two binding sites were missing from the sequence of the enzyme, however, tRNA would not find an appropriate site to interact

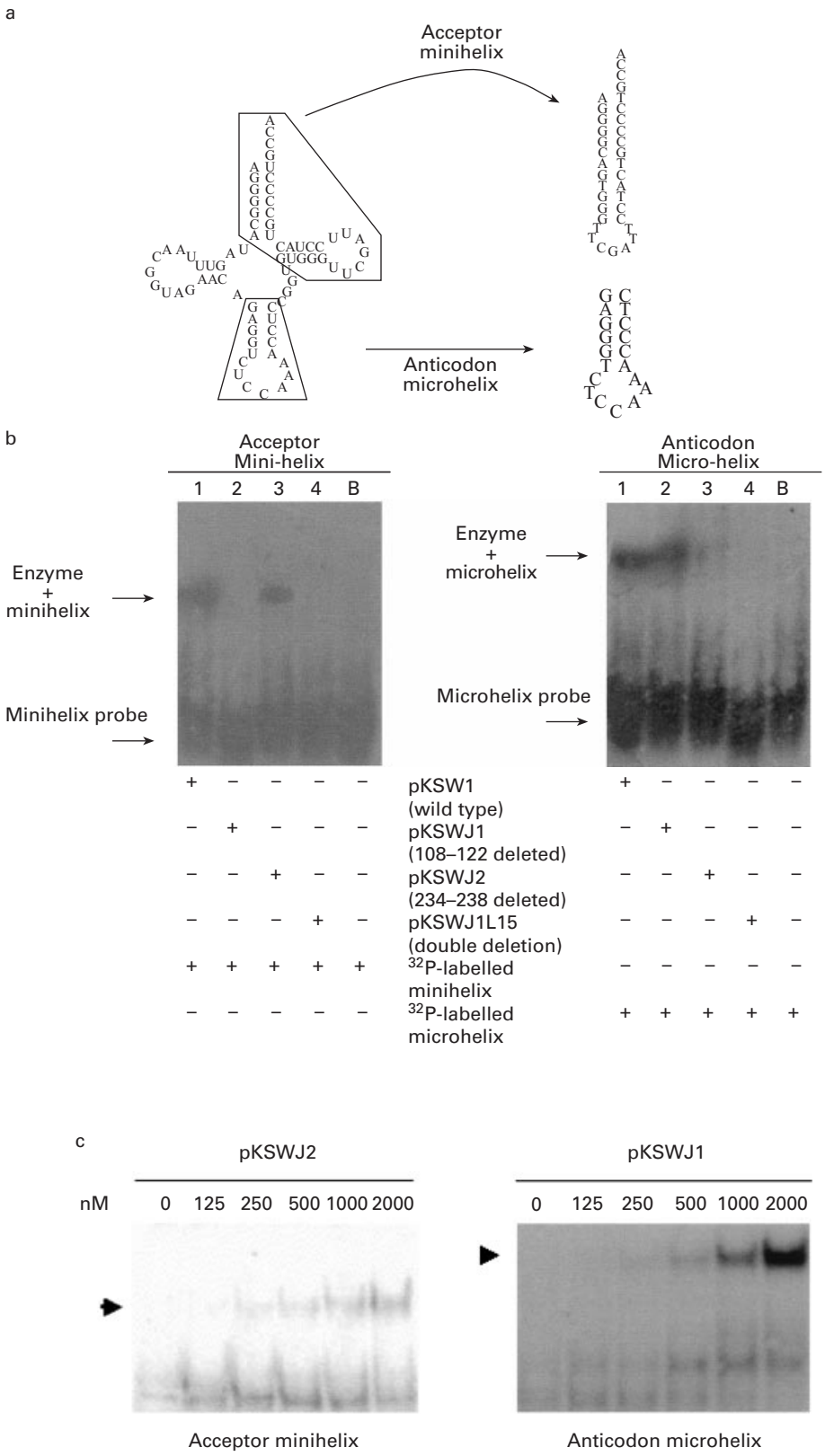

Figure 5 Gel-retardation showed the shift bands

The wt TrpRS (pKSW1) and the three mutant TrpRSs, pKSWJ1 (108–122 residues deleted), pKSWJ2 (234–238 residues deleted), and pKSWJ1L15 (both regions deleted), interacted with $tRNA^{Trp}$ elements analogue-tDNA minihelix or microhelix. (**a**) Sequence and clover leaf structure of *B. subtilis* $tRNA^{Trp}$ and sequence and hairpin structure of tDNA-acceptor minihelix and anticodon microhelix. (**b**) The arrows show the positions of the ^{32}P-labelled probes and the bands that were protein bound to the radiolabelled minihelix or microhelix. Lane 1, pKSW1 (wt); lane 2, pKSWJ1; lane 3, pKSWJ2; lane 4, pKSWJ1L15; B, blank (labelled probe only). The assay was performed with a constant 40 pmol of ^{32}P-labelled minihelix and microhelix in the presence of 4 μM TrpRS (wt or mutant). (**c**) Band-shift assay performed with ^{32}P-labelled minihelix and microhelix in the presence of 125–2000 nM mutant TrpRS, either encoded by pKSWJ1 or pKSWJ2. Arrows mark the protein complex with the tDNA-mini or microhelix.

with *B. subtilis* TrpRS and the further step of tRNA aminoacylation was interrupted.

The construction of the pKSW1 plasmid has resulted in a high-level production of *B. subtilis* TrpRS in *E. coli* cells [23]. This provided an optimal system for the production and mutagenic analysis of its *trpS* gene product. However, the analysed mutant proteins showed different properties during expression in cell cultures under IPTG-induced conditions. It can be assumed that residues 234–238 are very important, not only to tRNA binding but also to the structural stability. The deletion of residues 108–122, which removes 10 more amino acid residues from TrpRS than the amino acids 234–238 deletion, did not affect TrpRS expression; the mutants were still soluble proteins in normal cultures. Once residues 234–238 were deleted from the *trpRS* gene, however, the products of TrpRS mutant became an inclusion body. It puzzled us that residues 234–238 were located in a flexible loop in the TrpRS crystal [18,20,21]; the deletion of these amino acids should not have evident effects on TrpRS structure, unless it changes the balance of polarity on the surface of TrpRS. We thought, perhaps, that K236 plays a crucial role in the formation of TrpRS, because K236 is very conserved in TrpRSs from different sources. Furthermore, Lys has a second amino group at the ϵ position on its aliphatic chain which means it should contribute to the microenvironment of TrpRS. This hypothesis needs to be verified.

In conclusion, we have demonstrated for the first time in the present study, using biochemical methods, that residues 108–122 and residues 234–238 are tRNA-binding domains in *B. subtilis* TrpRS. The homology modelling and $tRNA^{Trp}$ aminoacylation kinetics parameters have shown that these are two vital domains that have direct effects on $tRNA^{Trp}$ binding and recognition. Residues 108–122 were considered as an acceptor-binding loop that allows sequence-specific interactions with identity elements in the $tRNA^{Trp}$ acceptor helix. Residues 234–238 provided a binding site to the anticodon of tRNA. These two domains of the synthetase keep the stability and accuracy of L-shaped tRNA binding. The tRNA-binding domain exists near the ATP-binding pocket, which facilitates the acyl group transfer from Trp-5′-AMP to cognate tRNA. All these results support the former hypotheses derived from the 2.9 Å crystal structures of ligand-free *B. stearothermophilus* TrpRS [17]. These two short regions are essential to tRNA recognition and binding. Their communication also needs the help of other residues in the TrpRS. A whole $tRNA^{Trp}$ molecule primarily interacts with these two regions, including residues 108–122 and 234–238, which forms a binding pocket with the help of other residues. This is supported by the K_m/k_{cat} values obtained for mutant enzymes in the $tRNA^{Trp}$ aminoacylation assay.

We thank Professor C. W. Carter, Jr. for the crystal data of *B. stearothermophilus* TrpRS, Dr X. Hong for the plasmid pKSW1, and Professor C. Wang and Professor D. Liu for their critical comments on the manuscript. This work was supported by the National Natural Science Foundation of China (Grant 39730120), Chinese Academy of Sciences (Grant KSCX2-2-04) and a Science-developing grant from the Science and Technology Commission of the Municipality.

REFERENCES

1 Cusack, S. (1995) Eleven down and nine to go. Nat. Struct. Biol. **2**, 824–831
2 Webster, T., Tsai, H., Kula, M., Mackie, G. A. and Schimmel, P. (1984) Specific sequence homology and three-dimensional structure of an aminoacyl transfer RNA synthetase. Science (Washington, D.C.) **226**, 1315–1317
3 Eriani, G., Delarue, M., Poch, O., Gangloff, J. and Moras, D. (1990) Partition of tRNA synthetases into two classes based on mutually exclusive sets of sequence motifs. Nature (London) **347**, 203–206
4 Cusack, S., Berthet-Colominas, C., Hartlein, M., Nassar, N. and Leberman, R. (1990) A second class of synthetase structure revealed by X-ray analysis of *Escherichia coli* seryl-tRNA synthetase at 2.5 A. Nature (London) **347**, 249–255
5 Rould, M. A., Perona, J. J., Söll, D. and Steitz, T. A. (1989) Structure of *E. coli* glutaminyl-tRNA synthetase complexed with tRNA(Gln) and ATP at 2.8 Å resolution. Science (Washington, D.C.) **246**, 1135–1142
6 Cavarelli, J., Eriani, G., Rees, B., Ruff, M., Boeglin, M., Mitschler, A., Martin, F., Gangloff, J., Thierry, J. C. and Moras, D. (1994) The active site of yeast aspartyl-tRNA synthetase: structural and functional aspects of the aminoacylation reaction. EMBO J. **13**, 327–337
7 Schimmel, P., Giegé, R., Moras, D. and Yokoyama, S. (1993) An operational RNA code for amino acids and possible relationship to genetic code. Proc. Natl. Acad. Sci. U.S.A. **90**, 8763–8768
8 Schimmel, P. and Ribas de Pouplana, L. (1995) Transfer RNA: from minihelix to genetic code. Cell (Cambridge, Mass.) **81**, 983–986
9 Ladner, J. E., Jack, A., Robertus, J. D., Brown, R. S., Rhodes, D., Clark, B. F. and Klug, A. (1975) Structure of yeast phenylalanine transfer RNA at 2.5 Å resolution. Proc. Natl. Acad. Sci. U.S.A. **72**, 4414–4418
10 Rich, A. and Schimmel, P. (1977) Structural organization of complexes of transfer RNAs with aminoacyl transfer RNA synthetases. Nucleic Acids Res. **4**, 1649–1665
11 Kim, S. H., Quigley, G. J., Suddath, F. L., McPherson, A., Sneden, D., Kim, J. J., Weinzierl, J. and Rich, A. (1973) Three-dimensional structure of yeast phenylalanine transfer RNA: folding of the polynucleotide chain. Science (Washington, D.C.) **179**, 285–288
12 Kim, S. H., Suddath, F. L., Quigley, G. J., McPherson, A., Sussman, J. L., Wang, A. H., Seeman, N. C. and Rich, A. (1974) Three-dimensional tertiary structure of yeast phenylalanine transfer RNA. Science (Washington, D.C.) **185**, 435–440
13 Steer, B. A. and Schimmel, P. (1999) Domain-domain communication in a miniature archaebacterial tRNA synthetase. Proc. Natl. Acad. Sci. U.S.A. **96**, 13644–13649
14 Webster, T. A., Lathrop, R. H. and Smith, T. F. (1987) Prediction of a common structural domain in aminoacyl-tRNA synthetases through use of a new pattern-directed inference system. Biochemistry **26**, 6950–6957
15 Hountondji, C., Dessen, P. and Blanquet, S. (1986) Sequence similarities among the family of aminoacyl-tRNA synthetases. Biochimie **68**, 1071–1078
16 Doublié, S., Bricogne, G., Gilmore, C. J. and Carter, Jr, C. W. (1995) Tryptophanyl-tRNA synthetase crystal structure reveals an unexpected homology to tyrosyl-tRNA synthetase. Structure **3**, 17–31
17 Ilyin, V. A., Temple, B., Hu, M., Li, G., Yin, Y., Vachette, P. and Carter, Jr, C. W. (2000) 2.9 Å crystal structure of ligand-free tryptophanyl-tRNA synthetase: domain movements fragment the adenine nucleotide binding site. Protein Sci. **9**, 218–231
18 Chow, K. C., Xue, H., Shi, W. and Wong, J. T.-F. (1992) Mutational identification of an essential tryptophan in tryptophanyl-tRNA synthetase of *Bacillus subtilis*. J. Biol. Chem. **267**, 9146–9149
19 Hogue, C. W. V., Doublié, S., Xue, H., Wong, J. T., Carter, Jr, C. W. and Szabo, A. G. (1996) A concerted tryptophanyl-adenylate-dependent conformational change in *Bacillus subtilis* tryptophanyl-tRNA synthetase revealed by the fluorescence of Trp92. J. Mol. Biol. **260**, 446–466
20 Sever, S., Rogers, K., Rogers, M. J., Carter, Jr, C. W. and Söll, D. (1996) *Escherichia coli* tryptophanyl-tRNA synthetase mutants selected for tryptophan auxotrophy implicate the dimer interface in optimizing amino acid binding. Biochemistry **35**, 32–40
21 Chow, K. C. and Wong, J. T.-F. (1988) Cloning and nucleotide sequence of the structural gene coding for *Bacillus subtilis* tryptophanyl-tRNA synthetase. Gene **73**, 537–543
22 Shi, W., Chow, K. C. and Wong, J. T.-F. (1990) High-level expression of *Bacillus subtilis* tryptophanyl-tRNA synthetase in *Escherichia coli*. Biochem. Cell Biol. **68**, 492–495
23 Xu, Z. J., Love, M. L., Ma, L. Y. Y., Blum, M., Bronskill, P. M., Bernstein, J., Grey, A. A., Hofmann, T., Camerman, N. and Wong, J. T.-F. (1989) Tryptophanyl-tRNA synthetase from *Bacillus subtilis*. Characterization and role of hydrophobicity in substrate recognition. J. Biol. Chem. **264**, 4304–4311
24 Jørgensen, R., Søgaard, T. M. M., Rossing, A. B., Martensen, P. M. and Justesen, J. (2000) Identification and characterization of human mitochondrial tryptophanyl-tRNA synthetase. J. Biol. Chem. **275**, 16820–16826
25 Chen, L., Jiang, G., Jin, Y. X. and Wang, D. B. (2001) Homology modelling of *Bacillus subtilis* Tryptophanyl-tRNA synthetase. Acta Biochim. Biophys. Sinica **33**, 687–690
26 Dieffenbach, C. W. and Dveksler, G. S. (1995) PCR Primer: A Laboratory Manual. Primer design, pp. 131–172, Cold Spring Harbor Press, New York
27 Xu, F., Jia, J., Jin, Y. X. and Wang, D. B. (2001) High-level expression and single-step purification of human tryptophanyl-tRNA synthetase. Protein Express. Purif. **23**, 296–300

28 Xu, F., Chen, X. L., Chen, L., Jin, Y. X. and Wang, D. B. (2001) Species-specific differences in the operational RNA code for aminoacylation of tRNA(Trp). Nucleic Acids Res. **29**, 4125–4133
29 Kaminska, M., Deniziak, M., Kerjan, P., Barciszewski, J. and Mirande, M. (2000) A recurrent general RNA binding domain appended to plant methionyl-tRNA synthetase acts as a cis-acting cofactor for aminoacylation. EMBO J. **19**, 6908–6917
30 Jahn, M., Rogers, M. J. and Söll, D. (1991) Anticodon and acceptor stem nucleotides in tRNA(Gln) are major recognition elements for *E. coli* glutaminyl-tRNA synthetase. Nature (London) **352**, 258–260
31 Pütz, J., Puglisi, J. D., Florentz, C. and Giegé, R. (1991) Identity elements for specific aminoacylation of yeast tRNA(Asp) by cognate aspartyl-tRNA synthetase. Science (Washington, D.C.) **252**, 1696–1699

Received 23 January 2002/16 April 2002; accepted 19 April 2002
Published as BJ Immediate Publication 19 April 2002, DOI 10.1042/BJ20020141